

The Activation of M₁ Muscarinic Receptor Signaling Induces Neuronal Differentiation in Pyramidal Hippocampal Neurons^S

Kathryn L. VanDeMark, Marina Guizzetti, Gennaro Giordano, and Lucio G. Costa

Department of Environmental and Occupational Health Sciences, University of Washington, Seattle, Washington (K.L.V., M.G., G.G., L.G.C.); and Department of Human Anatomy, Pharmacology, and Forensic Sciences, University of Parma Medical School, Parma, Italy (L.G.C.)

Received December 19, 2008; accepted February 2, 2009

ABSTRACT

Muscarinic receptors have been proposed to play an important role during brain development by regulating cell survival, proliferation, and differentiation. This study investigated the effect of muscarinic receptor activation on prenatal rat hippocampal pyramidal neuron differentiation and the signal transduction pathways involved in this effect. The cholinergic agonist carbachol, after 24 h in vitro, increased the length of the axon, without affecting the length of minor neurites. Carbachol-induced axonal growth was also observed in pyramidal neurons from the neocortex but not in granule neurons from the cerebellum. The effect of carbachol was mediated by the M₁ subtype of muscarinic receptors. The Ca²⁺ chelator 1,2-bis(2-aminophenoxy)ethane-*N,N,N',N'*-tetraacetic acid-acetoxymethyl ester, the two protein kinase C (PKC) inhibitors 3-[1-[3-(dimethylaminopropyl)-1*H*-indol-3-yl]-4-(1*H*-indol-3-yl)-1*H*-pyrrole-2,5-dione monohydrochloride (GF109203X) and 2-[8-[(dimethylamino)methyl]-6,7,8,9-tet-

rahydropyridol[1,2-*a*]indol-3-yl]-3-(1-methylindol-3-yl)maleimide (Ro-32-0432), and the extracellular signal-regulated kinase (ERK)1/2 inhibitors 2'-amino-3'-methoxyflavone (PD98059) and 1,4-diamino-2,3-dicyano-1,4-bis(methylthio)butadiene (U0126) all blocked carbachol-induced axonal outgrowth. In addition, down-regulation of ERK1/2 with small interfering RNA abolished the neuritogenic effect of carbachol. These data suggest an involvement of Ca²⁺, PKC, and ERK1/2 in carbachol-induced axonal growth. Carbachol indeed increased the release of Ca²⁺ from intracellular stores and induced PKC and ERK1/2 activation. Additional experiments showed that PKC, but not Ca²⁺, is involved in carbachol-induced ERK1/2 activation. Together, these results show that cholinergic stimulation of prenatal hippocampal pyramidal neurons accelerates axonal growth through the induction of Ca²⁺ mobilization and the activation of PKC and especially of ERK1/2.

This work was supported in part by the National Institutes of Health [Grants AA08154, ES07033, ES07032].

K.L.V. and M.G. contributed equally to this work.

The data presented here have in part appeared in abstract form as follows: VanDeMark K, Guizzetti M, Giordano G, and Costa LG (2006) Effect of ethanol on carbachol-induced neurite outgrowth in prenatal hippocampal neurons, in *Proceedings of the 45th Meeting of the Society of Toxicology*; 2006 March 5-9; San Diego, CA. Society of Toxicology, Reston, VA; VanDeMark KL, Guizzetti M, Giordano G, and Costa LG (2008) Ethanol inhibits carbachol-induced axon outgrowth in hippocampal neurons by inhibiting ERK1/2, in *Proceedings of the 47th Annual Meeting of the Society of Toxicology*; 2008 March 16-20; Seattle, WA, Society of Toxicology, Reston, VA; and VanDeMark KL, Guizzetti M, Giordano G, and Costa LG (2008) Ethanol inhibits hippocampal neuron differentiation induced by carbachol, in *2008 Joint ISBRA/RSA Scientific Conference*; 2008 June-2 July; Washington, DC, International Society for Biomedical Research on Alcoholism, Denver, CO, and Research Society on Alcoholism, Austin, TX.

Article, publication date, and citation information can be found at <http://jpet.aspetjournals.org>.

doi:10.1124/jpet.108.150128.

^SThe online version of this article (available at <http://jpet.aspetjournals.org>) contains supplemental material.

Neuronal differentiation is an essential event in brain development and begins with the sprouting of neurites followed by the elongation of axons and dendrites. Neuronal axons can project over very long distances to reach their final targets. Growth cones, located at the edges of growing axons and dendrites, are directed by extracellular cues that can repel or attract neurite growth in a given direction. These cues can be contact-mediated or soluble, secreted molecules. Contact-mediated molecules include extracellular matrix proteins and cell adhesion molecules; soluble molecules include neurotrophins and growth factors that activate several signal transduction pathways leading to the rearrangement of cytoskeletal proteins. Several of the signals directing neurite outgrowth derive from glial cells surrounding neurons, whereas others can derive from neurons themselves (Tessier-Lavigne and Goodman, 1996).

ABBREVIATIONS: PKC, protein kinase C; ERK, extracellular signal-regulated kinase; DMEM, Dulbecco's modified Eagle's medium; FBS, fetal bovine serum; MAP, microtubule-associated protein; Fluo-3/AM, 1-[2-amino-5-(2,7-dichloro-6-hydroxy-3-oxo-3*H*-xanthen-9-yl)]-2-(2'-amino-5'-methylphenoxy)ethane-*N,N,N',N'*-tetraacetic acid pentaacetoxymethyl ester; BAY-11, 3-[(4-methylphenyl)sulfonyl]-2-propenenitrile; BAPTA-AM, 1,2-bis(*o*-aminophenoxy)ethane-*N,N,N',N'*-tetraacetic acid tetra (acetoxymethyl) ester; U0126, 1,4-diamino-2,3-dicyano-1,4-bis(2-aminophenylthio)butadiene; PD98059, 2'-amino-3'-methoxyflavone; LY 294002, 2-(4-morpholinyl)-8-phenyl-4*H*-1-benzopyran-4-one; Gö 6976, 12-(2-cyanoethyl)-6,7,12,13-tetrahydro-13-methyl-5-oxo-5*H*-indolo(2,3-*a*)pyrrolo(3,4-*c*)-carbazole; siRNA, small interfering RNA; HBSS, Hanks' balanced salt solution; ACM, astrocyte-conditioned medium; CGC, cerebellar granule cell; MTT, thiazolyl blue tetrazolium bromide; CNS, central nervous system; IP₃, inositol trisphosphate; DAG, diacylglycerol; GF109203X, 3-[1-[3-(dimethylaminopropyl)-1*H*-indol-3-yl]-4-(1*H*-indol-3-yl)-1*H*-pyrrole-2,5-dione monohydrochloride; Ro-32-0432, 2-[8-[(dimethylamino)methyl]-6,7,8,9-tetrahydropyridol[1,2-*a*]indol-3-yl]-3-(1-methylindol-3-yl)maleimide; PI3K, phosphatidylinositol 3-kinase; PLD, phospholipase D; p70S6kinase, 70-kDa ribosomal S6 kinase; NF- κ B, nuclear factor- κ B.

There is substantial evidence that acetylcholine may influence various aspects of brain development. Components of the cholinergic system, including choline acetyltransferase and acetylcholine receptors, are present prenatally in several species, including rodents and humans, long before the appearance of synapses. Acetylcholine may have nontransmitter effects during development, because it can regulate morphogenic cell movements during gastrulation, glial cell proliferation, and neuronal differentiation and survival in the developing central nervous system (Lauder and Schambra, 1999; Hohmann, 2003). The observation that developing neurons may fire action potentials and trigger acetylcholine secretion from the axonal growth cone while the axon is still growing supports a role for acetylcholine in brain development (Yao et al., 2000).

Intrinsic cholinergic neurons are found in numerous brain regions, including the cerebral neocortex and the hippocampus, although most of the brain receives cholinergic innervations through projecting cholinergic axons originated in the basal forebrain and in the pontomesencephalon (Karczmar, 2007). The disruption of basal forebrain neurons during development results in delays in cortical neuron development and alterations in cortical morphology, as well as deficiencies in attention and memory (Berger-Sweeney, 2003).

The stimulation of neuronal muscarinic receptors has been shown to induce neurite outgrowth in chick dorsal root ganglia (Tata et al., 2003), neuroblastoma cells (De Jaco et al., 2002), and in a rat pheochromocytoma neuronal cell line (PC12) transfected with the M₁ muscarinic receptor (Pinkas-Kramarski et al., 1992). In addition, acetylcholine induces expression of genes associated with neuronal differentiation in PC12M1 cells (Pinkas-Kramarski et al., 1992). In the developing retina, acetylcholine released by amacrine cells evokes Ca²⁺ release and stabilizes developing dendrites in retinal ganglion cells (Lohmann et al., 2002).

Other neurotransmitters have also been implicated in the modulation of axonal growth. Glutamate, acting through N-methyl-D-aspartate receptors, induces neurite outgrowth in hippocampal neurons (Mattson et al., 1988) and cerebellar granule cells (Pearce et al., 1987). GABA promotes neurite outgrowth in rat cerebellar neurons (Michler, 1990), rat hippocampal neurons (Barbin et al., 1993), and rat olfactory bulb neurons cocultured with astrocytes (Matsutani and Yamamoto, 1998) via activation of GABA_A receptors and of mouse olfactory receptor neurons (Priest and Puche, 2004) via GABA_B receptors. Together, these observations strongly suggest that neurotransmitters, including acetylcholine, may play an important role during brain development and, particularly, in neurite outgrowth.

The first goal of this study was to investigate the effect of cholinergic stimulation on neurite outgrowth in fetal hippocampal pyramidal neurons in vitro. The morphological differentiation of hippocampal neurons in vitro has been well characterized. Neurons begin by extending several minor processes; one of these processes begins to grow faster than other processes and expresses axon-specific markers (such as Tau); at this stage (that is reached approximately after 24–48 h in vitro), the pyramidal neuron occurs as a polarized cell with an axon and several minor neurites. The remaining processes develop into dendrites, expressing specific dendritic markers, at a later time (Dotti et al., 1988).

The second goal of this study was to characterize the intracellular pathway responsible for the effect of cholinergic

stimulation on hippocampal neuron neurite outgrowth. We found that the axons of hippocampal neurons in culture exposed to the cholinergic agonist carbachol extended more rapidly than the axons from control cultures. The effect of carbachol was mediated by M₁ muscarinic receptors that induced Ca²⁺ release from the intracellular stores and activation of protein kinase C (PKC) and extracellular signal-regulated kinase (ERK) 1/2.

Materials and Methods

Materials. Time-pregnant Sprague-Dawley rats were purchased from Taconic Farms (Hudson, NY). Neurobasal-A medium, Dulbecco's modified Eagle's medium (DMEM), fetal bovine serum (FBS), and trypsin were from Invitrogen (Carlsbad, CA). Cell culture inserts and nylon mesh filters were from BD Biosciences (Franklin Lakes, NJ); glass coverslips were from Fisher Scientific (Federal Way, WA), and plastic coverslips were from Nalge Nunc (Rochester, NY). The antibodies against tubulin β III isoform, microtubule-associated protein (MAP) 2, and Tau were purchased from Millipore Bioscience Reagents (Temecula, CA); the Alexa Fluor 488 and 555 secondary antibodies, Hoechst 33342 dye, and 1-[2-amino-5-(2,7-dichloro-6-hydroxy-3-oxo-3H-xanthen-9-yl)]-2-(2'-amino-5'-methylphenoxy)ethane-N,N,N',N'-tetraacetic acid pentaacetoxymethyl ester (Fluo-3/AM) were purchased from Invitrogen (Carlsbad, CA). Antibodies against phospho-ERK1/2 and ERK1/2 were purchased from Cell Signaling Technology Inc. (Danvers, MA). All PKC inhibitors, BAY-11, 1,2-bis(o-aminophenoxy)ethane-N,N,N',N'-tetraacetic acid tetra (acetoxymethyl) ester (BAPTA-AM), U0126, PD98059, LY 294002, rapamycin [23,27-epoxy-3H-pyrido(2,1-c)(1,4)oxaazacyclohentriacontine], and wortmannin [1,6b β ,7,8,9a,10,11,11b-octahydro-11-hydroxy-1-(methoxymethyl)-9a β ,11b β -dimethyl-3H-furo[4,3,2-de]indeno[4,5-h][2]benzopyran-3,6,9-trione acetate] were all purchased from Calbiochem (Gibbstown, NJ). Amaxa Primary Rat Neucleofector kit was purchased from Amaxa Biosystems (Gaithersburg, MD), and siRNA was purchased from Dharmacon RNA Technologies (Lafayette, CO). The PepTag Assay for NonRadioactive Detection of PKC was from Promega (Madison, WI). Carbachol, anti-glutamyl antibody, and all other reagents were purchased from Sigma-Aldrich (St. Louis, MO).

Hippocampal Neuron Culture. Primary cultures of hippocampal neurons were prepared from 21-day-old rat fetuses as described previously (Brewer et al., 1993), with minor modifications. In brief, a pregnant dam was euthanized with carbon dioxide, and the uterine horns were removed by using a protocol approved by the University of Washington Institutional Animal Care and Use Committee. Fetuses were removed and sacrificed by decapitation. The hippocampi were removed from the cerebral hemispheres, stripped of meninges, dissected into 1- to 2-mm³ pieces in Hanks' balanced salt solution (HBSS), and treated with papain (2 mg/ml HBSS) in the presence of DNase (40 μ g/ml) and MgCl (5 mM) for 30 min at 37°C. The tissue was spun down and resuspended in Neurobasal-A complete media (Neurobasal-A medium supplemented with 10% FBS, 30 mM glucose, 3 mM GlutaMAX (Invitrogen), 1% gentamicin, and 0.5% fungizone) and DNase (40 μ g/ml). Tissue was further dissociated by repeated passages through a Pasteur pipette, and cells were filtered through a nylon mesh of 40- μ m pore size. Cells were then spun down and resuspended in Neurobasal-A complete media. For the neurite extension assays, cells were seeded on cell culture porous inserts at the density 2×10^5 per insert. For morphometric analysis, cells were seeded on round glass coverslips placed in 24-well plates at 1×10^4 cells per coverslip. Inserts and coverslips were coated overnight with 100 μ g/ml poly-D-lysine at 37°C. Neurons were allowed to attach in Neurobasal-A complete media for 30 min, after which they were switched to astrocyte-conditioned medium (ACM) containing the various treatments for 24 h. No differences in cell survival were noticed between neurons maintained for 24 h in ACM compared with cells maintained in Neurobasal-A medium.

For Western blot analysis and PKC activity cells were plated in 35-mm dishes (2×10^6 cells/dish for Western blot experiments and 5×10^6 cells/dish for PKC activity assays). Cells were allowed to attach overnight in Neurobasal-A complete media and then switched to ACM containing the different treatments.

Neocortical Neuron Cultures. Primary neocortical neuron cultures were prepared from 21-day-old rat fetuses as described previously (Brewer et al., 1993). Neocortices were separated from the brain, and the meninges were removed. To remove glial cells, the final cell suspension was initially plated in poly-D-lysine-coated flasks (50 $\mu\text{g}/\text{ml}$) for 20 min. At the end of the incubation, the supernatant containing the unattached neurons was collected and plated on glass coverslips.

Cerebellar Granule Cell Cultures. Primary cerebellar granule cell (CGC) cultures were prepared from 7-day-old rat pups as described previously (Giordano et al., 2006). In brief, pups were sacrificed by decapitation. Cerebella were rapidly dissected from the brain in HBSS, and the meninges were removed. The tissue was cut into small pieces, enzymatically dissociated using 2 mg/ml papain in the presence of 40 $\mu\text{g}/\text{ml}$ DNase for 30 min at 37°C, and then mechanically dissociated using a long-stem Pasteur pipette. The cell suspension was then centrifuged at 300g for 5 min at 4°C, and the pellet was resuspended in complete growth medium consisting of Neurobasal-A media containing 1 mM GlutaMAX, gentamicin, and FBS (10%), and neurons were seeded on round glass coverslips.

Preparation of Astrocyte-Conditioned Medium. Primary astrocyte cultures were prepared from cerebral cortex of 21-day-old rat fetuses as described previously (Guizzetti et al., 1996) and maintained for 10 to 14 days in DMEM/10% FBS. Cells were passed in 100-mm dishes and cultured for 4 days in DMEM/10% FBS. Astrocytes were then switched to DMEM supplemented with 0.1% bovine serum albumin for 48 h at the end of which the medium was collected and spun for 10 min at 200g to remove any debris and floating cells. This medium was used for neuron treatments.

Neurite Extension Assay. Neurite extension was assessed spectrophotometrically following a previously described method (Smit et al., 2003). In brief, at the end of the 24-h treatment, neurons plated on cell culture porous inserts were fixed with ice-cold methanol and stained with 0.09% cresyl violet dye. Cell bodies that were plated on the top side of the porous inserts were dissociated and removed from the neurites that had grown through the pores to the underside of the insert using a cotton swab. The dye associated with neuritic proteins was solubilized with an extraction buffer, and the absorbance was measured at 562 nm using a SPECTRAMax PLUS microplate spectrophotometer (Molecular Devices, Sunnyvale, CA).

Immunocytochemistry and Morphometric Analysis. Neurons plated on glass coverslips were treated for 24 h; the cells were fixed in 4% paraformaldehyde, permeabilized in 0.1% Triton X-100, and blocked in 3% bovine serum albumin for 30 min. The coverslips were then incubated for at least 18 h with the neuron-specific mouse anti- β III tubulin antibody (Millipore Bioscience Reagents). Neocortical cultures were stained an additional hour with rabbit anti-glutamate antibody (Sigma-Aldrich).

In some experiments, hippocampal neurons, fixed in 4% paraformaldehyde in the presence of 15% sucrose and blocked with fetal calf serum for 1 h, were coincubated with rabbit anti-MAP2 and mouse anti-Tau antibody (Millipore Bioscience Reagents). After primary antibody incubations, coverslips were incubated for 1 h with either Alexa Fluor 488 or Alexa Fluor 555; nuclei were then stained with 5 $\mu\text{g}/\text{ml}$ Hoescht dye. Coverslips were mounted onto glass slides with Vectashield mounting gel (Vector Laboratories, Burlingame, CA), covered with cover glasses (Corning Life Sciences, Acton, MA), and sealed with nail polish.

The slides were viewed with a fluorescence microscope (Nikon, Melville, NY), and pictures were obtained using a SPOT-RT digital camera (Diagnostic Instruments, Inc., Sterling Heights, MI). The images were analyzed with MetaMorph 6.1 (Molecular Devices). Hippocampal neuron analysis was limited to cells that were identi-

fiable as stage 3 pyramidal cells and were not in contact with any other cells. Stage 3 hippocampal pyramidal neurons were those with three or more extensions, a cell body diameter of 10 to 15 μm , two to five undifferentiated neurites, and a single axon with length $\geq 40 \mu\text{m}$ (Dotti et al., 1988).

Cortical pyramidal neurons were identified by glutamate staining that distinguishes them from the nonpyramidal, GABA-expressing neurons of the neocortex (Whitworth et al., 2002). The measurement of cerebellar granule cell neurites was carried out as described previously (Bearer et al., 1999). The neurite had to meet the following requirements: it must emerge from an isolated cell (not a clump of cells), it must not contact other cells or neurites, and it must be longer than the diameter of the cell body. Sixty cells from at least three experiments were measured in each condition.

Intracellular Calcium Measurement. Neurons plated in 35-mm glass-bottomed dishes were loaded with the Ca^{2+} -sensitive fluorescent dye Fluo-3/AM (3 μM) and placed on the stage of an inverted microscope. The dye in the cytoplasmic portion of the cells was excited, and fluorescence images were captured at 10-s intervals by a charge-coupled device camera (Princeton Scientific Instruments, Trenton NJ). Fifty cells in each treatment group were analyzed using MetaMorph software (Molecular Devices). Fluorescence measurements were normalized as $\Delta F/F$ ($F - F_0/F$; F was the intensity value obtained during the experiment, and F_0 was the baseline intensity value). Cells were classified as responders or nonresponders depending on the size of the carbachol-induced rise in intracellular calcium. Only cells responding with a 10% or greater rise in intracellular calcium were analyzed further. Parameters analyzed were the percentage of responding neurons and the average peak response.

Measurement of PKC Activity. Neurons, plated in 35-mm dishes, were grown overnight in Neurobasal-A complete followed by 5-, 15-, or 30-min treatments with carbachol in ACM. Cells were then lysed in extraction buffer (25 mM Tris, 0.05% Triton X-100, 10 mM β -mercaptoethanol, and protease and phosphatase inhibitors). The lysates were collected, sonicated, rocked for 40 min at 4°C, and centrifuged at 13,000g for 10 min. The resulting supernatant was collected, and protein content was determined in each sample by the Bradford method (Bradford, 1976). Equal amounts of protein were used in each PKC reaction following the PepTag Assay for NonRadioactive Detection of Protein Kinase C (Promega, Madison, WI). In brief, samples were incubated with a positively charged, fluorescent, PKC-specific peptide for 30 min. Mixtures were boiled for 10 min to stop the reaction and were separated on agarose gels. The phosphorylated, negatively charged peptide separated from the nonphosphorylated, positively charged peptide was visualized under UV light. Resulting bands were quantified by densitometry and normalized to controls.

Protein Isolation and Western Blot Analysis. Neurons, plated in 35-mm dishes, were grown overnight in Neurobasal-A complete media followed by 30-min treatments with carbachol in ACM. After treatment, cells were lysed with cell lysis buffer (20 mM Tris-HCl, 150 mM NaCl, 1 mM EDTA, 1 mM EGTA, 1% Triton, 0.25% SDS, 50 mM NaF, 12.5 Na pyrophosphate, 11 mM Na β -glycerophosphate, 2.5 mM sodium orthovanadate, and 1 $\mu\text{g}/\text{ml}$ leupeptin) supplemented with a protease inhibitor cocktail (Roche Diagnostics, Indianapolis, IN); proteins were extracted as described above; the protein content was quantified by the bicinchoninic acid protein assay (Pierce Chemical, Rockford, IL); and equal amounts of protein were loaded and separated in 10% Bis-Tris gels and transferred to polyvinylidene difluoride membranes. Membranes were blocked in 5% milk in Tris-buffered saline/Tween 20 and incubated with anti-phospho-ERK1/2 (Cell Signaling Technology Inc.), followed by a horseradish peroxidase-conjugated secondary antibody; the same membranes were stripped and reprobed for total ERK1/2 and β -actin. The resulting bands were quantified by densitometry and normalized to controls.

Transfection of Primary Hippocampal Neurons with ERK1/2 siRNA. Neurons were transfected as per the manufacturer's Optimized

Protocol for Primary Rat Hippocampal or Cortical Neurons (Nucleofector II; Amaxa Biosystems). In brief, immediately after isolation primary, neurons were resuspended in Nucleofector solution. Aliquots of neurons were mixed with or without ERK1 siRNA (0.4 μ M) plus ERK2 siRNA (0.4 μ M) or nontarget siRNA (0.8 μ M) and transfected using the Nucleofector program O-003. Cells were then transferred to RPMI 1640 medium (10% FBS and 2 mM GlutaMAX) and allowed to recover for 20 min at 37°C. The neurons were then plated on either glass coverslips or 35-mm dishes precoated with poly-D-lysine. After 4 h, the medium was changed to fresh RPMI 1640 medium (10% FBS and 2 mM GlutaMAX) overnight, and the cells were treated the next morning in ACM with or without carbachol (100 μ M) for 24 h. ERK1/2 down-regulation in ERK1/2 siRNA-transfected cells was verified by Western blot.

MTT Assay. Cell viability was measured using thiazolyl blue tetrazolium bromide (MTT). At the end of carbachol treatments, hippocampal neurons plated in 24-well plates (2×10^5 cells/well) were washed and incubated with 250 μ g/ml MTT in PBS for 1 h at 37°C followed by a 5-min wash in dimethyl sulfoxide to solubilize the MTT-formazan. The absorbance of the MTT-formazan complex was measured by spectrophotometer set to detect 562-nm wavelengths.

Statistical Analysis. Each experiment was carried out three times. In the morphometric analyses, at least 60 cells per treatment were measured. All statistical tests were carried out using Kaleida-Graph 4.0 (Abelbeck/Synergy, Reading, PA). One-way analysis of variance followed by the Dunnett's test was used to determine significant differences from controls. For two-group comparisons, Student's *t* test was used. Values are expressed as mean \pm S.E.M.

Results

Muscarinic Receptor Stimulation Induces Neurite Outgrowth in Primary Pyramidal Neurons. Stimulation of muscarinic receptors has been shown to induce neurite outgrowth in neuronal cell lines and peripheral neurons (Pinkas-Kramarski et al., 1992; De Jaco et al., 2002; Tata et al., 2003). We hypothesized that muscarinic receptor stimulation may also induce neurite outgrowth in CNS neurons. To verify this hypothesis, fetal hippocampal neurons were plated in transwell cell culture inserts containing a permeable membrane with 3- μ m pores at their base and placed into 24-well plates containing ACM in the presence or in the absence of different concentrations of the nonhydrolyzable cholinergic agonist carbachol (10 nM–1 mM) for 24 h. Proteins from the neurites growing on the underside of the porous membranes were quantified spectrophotometrically. ACM was used in all the experiments because astrocytes release factors that are essential for neuronal survival and represent a relatively physiological environment for neurons.

Carbachol caused a significant increase in hippocampal neurite outgrowth, with a maximal effect observed at 100 μ M (Fig. 1). At this concentration, a 2.5-fold increase in absorbance was measured over that of control cells. This effect was not because of an increase in survival of carbachol-treated neurons, as indicated by an MTT cell viability assay (data not shown).

Because the described method does not provide information regarding neuronal morphology, morphometric experiments were performed. Hippocampal neurons plated on glass coverslips and treated for 24 h with 1 to 100 μ M carbachol were immunolabeled with a neuron-specific β III-tubulin antibody and visualized under a fluorescence microscope. Morphometric analysis of neuronal extensions was carried out in stage 3 hippocampal neurons as defined previously (Dotti et al., 1988) and described under *Materials and Methods*, using

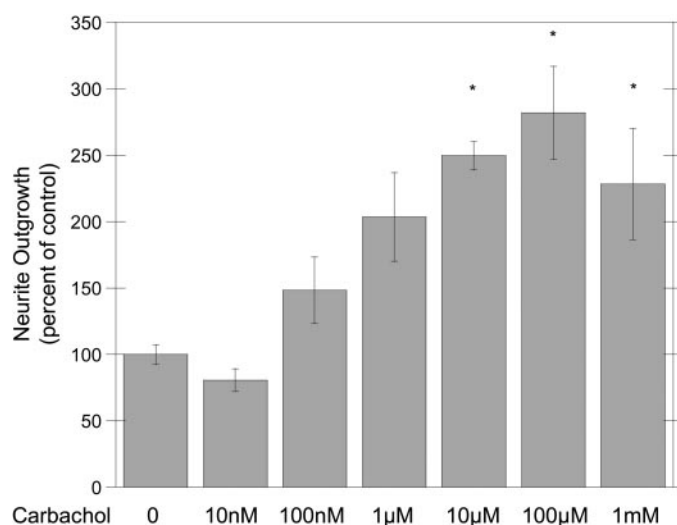


Fig. 1. Effect of carbachol on rat hippocampal neuron neurite outgrowth. Hippocampal neurons plated in porous inserts were incubated with or without 10 nM–1 mM carbachol for 24 h; neurite outgrowth was assessed spectrophotometrically, as described under *Materials and Methods*. Results are the average of three independent experiments and are expressed as mean \pm S.E.M. (*, $p < 0.05$ compared with control).

MetaMorph software. Carbachol caused an increase in the length of the longest neurite (Fig. 2A), whereas it did not affect the length of the minor neurites, nor the number of extensions per cell (Fig. 2, B and C). The percentage of cells with a neurite 150 μ m or longer increased by more than 2-fold after treatment with 100 μ M carbachol (Fig. 2D). Figure 2, E and F, shows representative fields of neurons from untreated and carbachol-treated cultures, respectively.

To verify the axonal identity of the longest neurites measured by morphometric analysis, hippocampal neurons were labeled with the dendritic marker MAP2, expressed in all neurites of nonpolarized stage 2 hippocampal neurons and in the minor neurites and the proximal part of the axons in stage 3 pyramidal cells, as well as the axon-specific marker Tau, expressed in the distal part of the axons in type 3 pyramidal neurons (Schwamborn et al., 2006). The majority of the cells morphologically recognizable as type 3 neurons expressed Tau-1 in their axons, indicating that carbachol induced the growth of the axon in hippocampal pyramidal neurons (data not shown). Figure 2G shows a representative field of pyramidal neurons costained for MAP2 (green) and Tau (red). The white arrow identifies a Tau-expressing type 3 pyramidal neuron.

To explore whether muscarinic or nicotinic receptors were involved in the neurotogenic effect of carbachol, hippocampal neurons seeded in porous inserts were treated with 100 μ M carbachol in the presence of the muscarinic antagonist atropine or the nicotinic antagonist mecamylamine, and neurite outgrowth was assessed spectrophotometrically. Mecamylamine (1–100 μ M) had no effect on carbachol-stimulated neurite outgrowth (Supplemental Fig. 1), whereas atropine abolished the effect of carbachol (Fig. 3A). To determine the muscarinic acetylcholine receptor subtype responsible for carbachol-stimulated neurite outgrowth, pirenzepine, methoctramine, *para*-fluoro-hexahydrosila-difenidol, and tropicamide, inhibitors of M₁–M₄ receptors, respectively, were used. Pirenzepine (1 μ M) strongly inhibited carbachol-stimulated hippocampal neurite outgrowth (Fig. 3A), whereas none of the

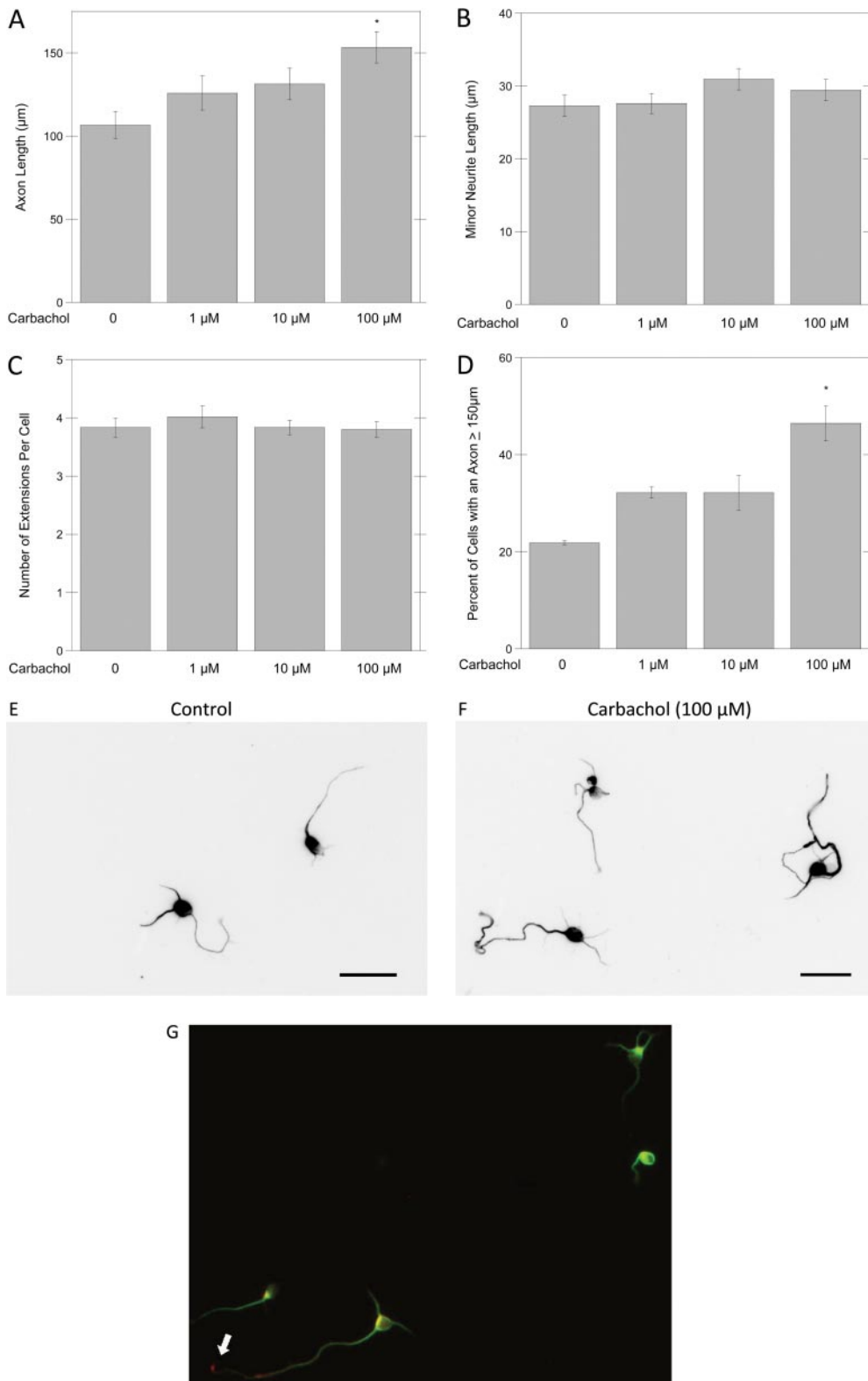


Fig. 2. Morphometric analysis of the effect of carbachol on neurite outgrowth in rat hippocampal neurons. Hippocampal neurons plated on coverslips were incubated with or without carbachol (1–100 μM) for 24 h. Cells were then fixed and stained with a β-tubulin antibody and a fluorescent secondary as described under *Materials and Methods*. Axon (A) and minor neurite (B) length was quantified using MetaMorph. C, number of extensions per cell. D, percentage of cells with an axon ≥ 150 μm. Representative fields of control (E) and carbachol-treated (F) hippocampal neurons are also shown. Magnification, 20 \times . Scale bar, 25 μm. The results derive from the measurements of 60 cells per treatment and are expressed as mean \pm S.E.M. (*, $p < 0.05$ compared with control). G, hippocampal neurons were labeled with the dendritic marker MAP2 (green) and the axon-specific marker Tau (red) (G). Magnification, 20 \times . The white arrow points to a stage 3 pyramidal neuron positive for Tau.

other subtype antagonists had any significant effect. These results were confirmed by morphometric analysis: pirenzepine (1 μM) inhibited carbachol-induced axonal growth, whereas the M_3 receptor inhibitor 4-diphenylacetoxy-*N*-methylpiperidine methiodide had no effect (Fig. 3B). These findings indicate that the effect of carbachol on hippocampal

neuron neurite outgrowth is mediated by the M_1 subtype of muscarinic receptors.

To determine whether the effect of carbachol was specific for hippocampal pyramidal neurons or whether other CNS neurons also responded to cholinergic stimulation, we tested the effect of carbachol on CGC and neocortical pyramidal

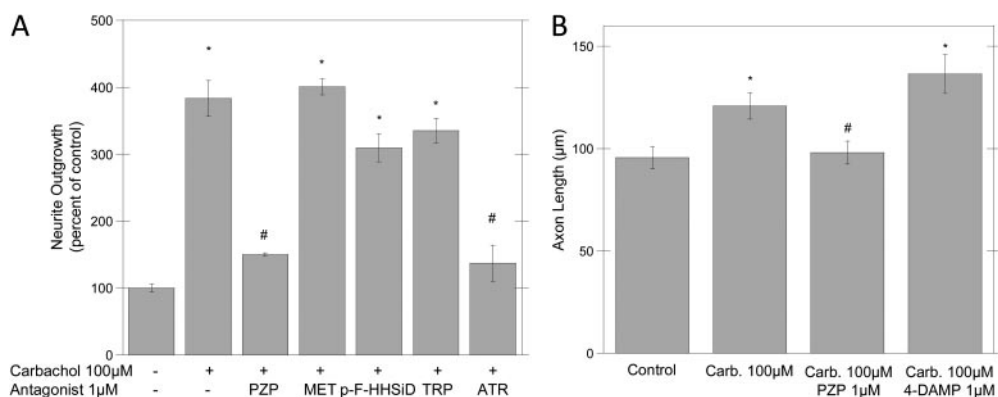


Fig. 3. Effect of muscarinic antagonists on carbachol-induced neurite outgrowth. A, hippocampal neurons plated on porous inserts were treated for 24 h with carbachol (100 μM) in the presence of the muscarinic receptor antagonist atropine (ATR), the M₁ muscarinic receptor antagonist pirenzepine (PZP), the M₂ antagonist methoctramine (MET), the M₃ antagonist *para*-fluoro-hexahydrosila-difenidol (p-F-HHSiD), or the M₄ antagonist tropicamide (TRP), all at 1 μM. Data are the average of six independent determinations. B, morphometric analysis of pyramidal hippocampal neurons treated with 100 μM carbachol in the presence of PZP or the M₃ antagonist 4-diphenylacetoxy-*N*-methylpiperidine methiodide (4-DAMP). The results derive from the measurements of 60 cells per treatment and are expressed as mean ± S.E.M. (*, $p < 0.05$ compared with control; #, $p < 0.05$ compared with carbachol).

neurons. Although neurons prepared from the cerebellum of 7-day-old rats are essentially a purified population of CGC, neocortical neurons can be divided into two morphologically and functionally distinct groups: pyramidal and nonpyramidal cells, with the pyramidal group constituting 70% of all the neurons in the cortex (DeFelipe and Fariñas, 1992). Because pyramidal neurons are excitatory glutamatergic neurons, they can be distinguished from the nonpyramidal, GABAergic neurons of the cortex by glutamate immunostaining. We found that carbachol did not affect the length of the neurites in CGCs, but it caused a significant increase in the axon length of neocortical glutamatergic stage 3 pyramidal cells positive to glutamate staining (Fig. 4, A and B). Figure 4, C and D, shows representative fields of neocortical neurons in control and carbachol-treated cultures. Taken together, these data indicate that muscarinic receptor stimulation induces axonal growth in hippocampal and cortical pyramidal neurons.

Intracellular Signaling Involved in Carbachol-Induced Axonal Growth in Hippocampal Pyramidal Neurons. To determine which signaling pathway may be involved in carbachol-induced axonal growth, hippocampal neurons were incubated with carbachol (100 μM) in the presence of various pharmacological inhibitors or Ca²⁺ chelators.

M₁, as well as M₃ and M₅, muscarinic receptors are coupled to G_q proteins that activate phospholipase C, leading to the formation of inositol trisphosphate (IP₃), that induces the release of Ca²⁺ from intracellular stores, and diacylglycerol (DAG), an activator of conventional and novel PKCs. Therefore, we tested the involvement of Ca²⁺ and PKC in carbachol-induced neurite outgrowth. When hippocampal neurons were incubated in the presence of the cell-permeable Ca²⁺ chelator BAPTA-AM, axonal outgrowth induced by carbachol was inhibited; in contrast, EGTA, a chelator of extracellular Ca²⁺ that does not cross the plasma membrane, did not inhibit the effect of carbachol, suggesting that Ca²⁺ released from intracellular stores is involved in the effect of carbachol on neurite outgrowth (Fig. 5A).

To test the involvement of PKC in carbachol-induced axonal growth, three different pharmacological inhibitors, inhibiting Ca²⁺- and/or DAG-dependent PKCs were used. The

pan-PKC inhibitor GF109203X (which inhibits PKCs α, βI, βII, γ, δ, and ε) and Ro-32-0432 (an inhibitor of PKCs α, βI, βII, γ, and ε) blocked carbachol-stimulated axonal growth, whereas Gö 6976 (an inhibitor of PKCs α and βI) had no effect (Fig. 5B). These data suggested that the Ca²⁺-dependent PKC βII and γ and/or Ca²⁺-independent PKC ε may be involved in the effect of carbachol on axonal growth.

We have previously reported that, in astrocytes, muscarinic receptors activate additional signaling pathways, including phosphatidylinositol 3-kinase (PI3K), phospholipase D (PLD), 70-kDa ribosomal S6 kinase (p70S6kinase), and nuclear factor-κB (NF-κB) (Costa et al., 2004). However, the PI3K inhibitors LY 294002 and wortmannin, the PLD inhibitor 1-butanol (its inactive analog *t*-butanol was used as a negative control), the p70S6kinase inhibitor rapamycin, and the NF-κB inhibitor BAY-11 were all ineffective at inhibiting carbachol-stimulated axonal growth (data not shown).

We also tested the role of ERK1/2 in carbachol-induced axon growth in hippocampal neurons, because these enzymes can be activated by G protein-coupled receptors and PKC and are known to be involved in neuronal differentiation (Naor et al., 2000; Song et al., 2005). Two different ERK1/2 inhibitors, U0126 and PD98059, antagonized carbachol-induced axonal growth (Fig. 6A).

To further confirm the involvement of ERK1/2 in carbachol-induced axonal growth, we down-regulated ERK1 and ERK2 protein expression using specific siRNAs (0.4 μM ERK1 siRNA and 0.4 μM ERK2 siRNA) transfected into neurons by Amaxa Nucleofector technology. In these experiments, we used two controls: the first control was represented by neurons that were electroporated in the absence of siRNA; the second control was represented by neurons electroporated in the presence of a nontarget siRNA (0.8 μM). The down-regulation of ERK1/2 expression in ERK1/2 siRNA-transfected neurons was confirmed by Western blot analysis (Fig. 6, B and C). Morphometric analysis revealed that although in neurons electroporated in the absence of siRNA and neurons electroporated in the presence of nontarget siRNA carbachol was able to increase axonal length, in neurons transfected with ERK1/2 siRNAs the effect of carbachol was abolished (Fig. 6D). These results suggest that the

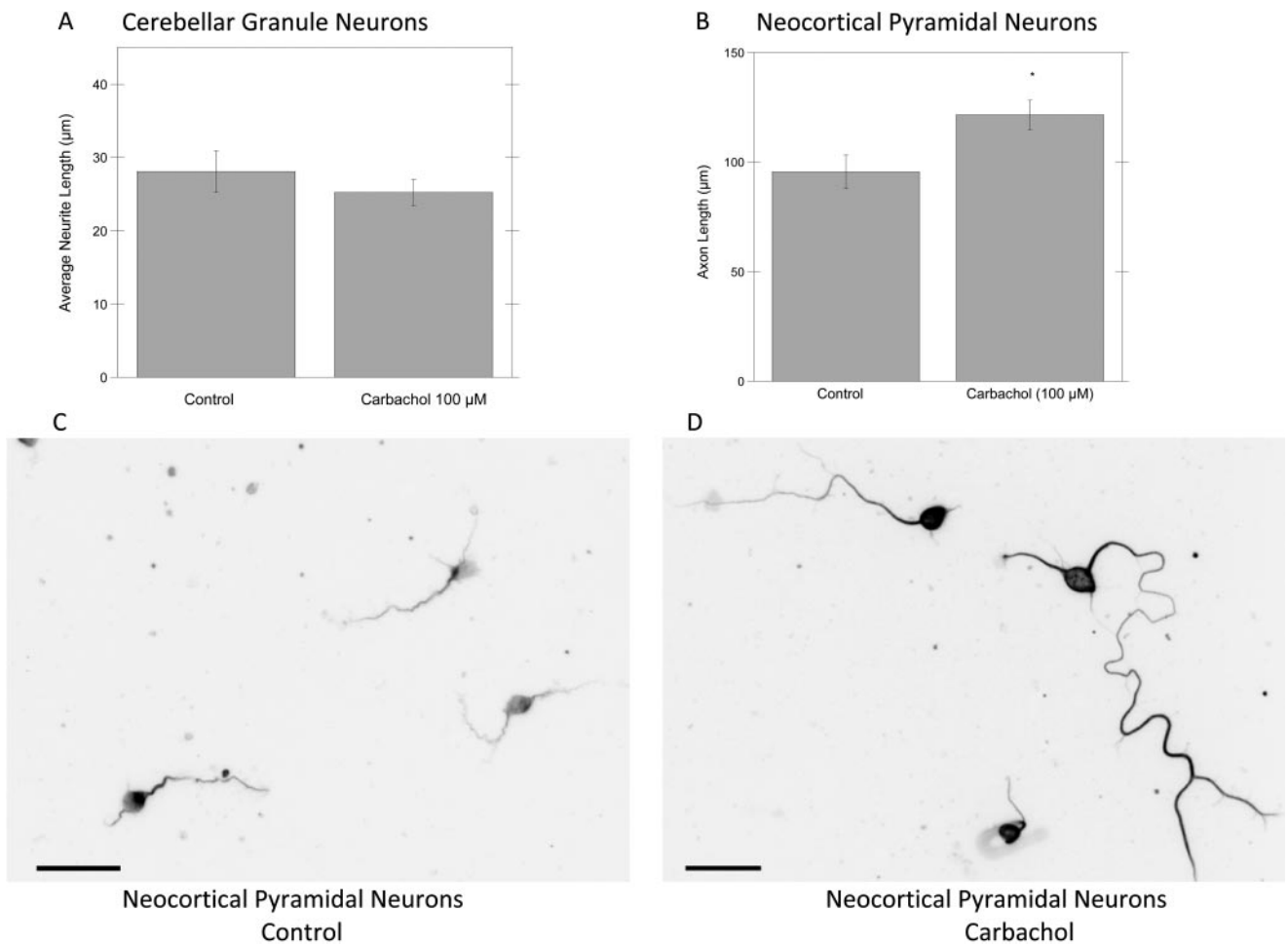


Fig. 4. Effect of carbachol on neurite outgrowth in cerebellar granule neurons and neocortical pyramidal neurons. CGN (A) and neocortical pyramidal neurons (B–D) plated on coverslips were incubated with or without 100 μ M carbachol for 24 h. Cells were then fixed and stained with a β -tubulin antibody and a fluorescent secondary; neocortical pyramidal neurons were also stained with an anti-glutamate antibody as described under *Materials and Methods*. Neurite length of CGC (A) and axon length in stage 3 pyramidal neocortical neurons (B) were quantified using MetaMorph. Representative fields of control (C) and carbachol-treated (D) neocortical pyramidal neurons. Magnification, 20 \times . Scale bars, 25 μ m. The results derive from the measurements of 60 cells per treatment per cell type. Results are expressed as mean \pm S.E.M. (*, $p < 0.05$ compared with control).

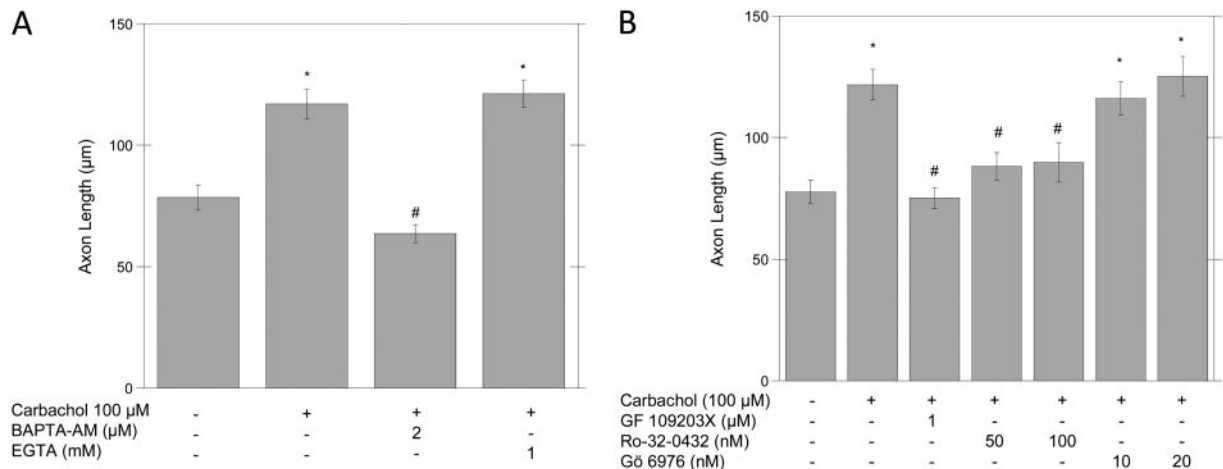


Fig. 5. Effect of pharmacological inhibitors of intracellular signaling pathways on carbachol-stimulated axonal growth. Hippocampal neurons plated on coverslips were treated with carbachol and the intracellular Ca^{2+} chelator BAPTA-AM, the extracellular Ca^{2+} chelator EGTA (A), the pan-PKC inhibitor GF109203X, and the semiselective PKC inhibitors Ro-32-0432 (inhibiting PKCs α , β I, β II, γ , and ϵ) and G6 6976 (inhibiting PKCs α and β I) (B) for 24 h. Cells were then fixed and stained with a β -tubulin antibody and a fluorescent secondary as described under *Materials and Methods*. The length of the axons was quantified using MetaMorph. The results derive from the measurements of 60 cells per treatment and are expressed as mean \pm S.E.M. (*, $p < 0.05$ versus control; #, $p < 0.05$ versus carbachol).

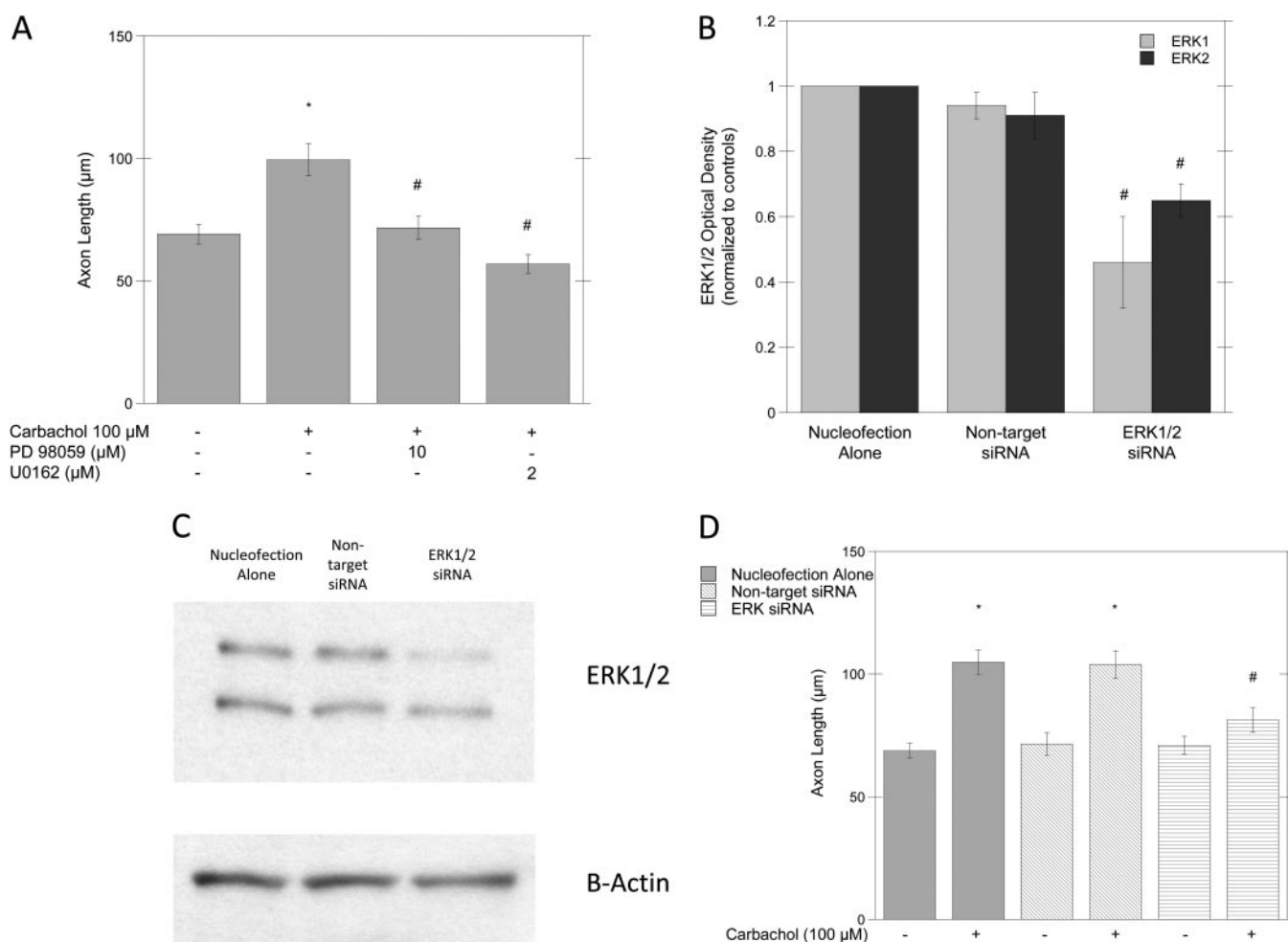


Fig. 6. Role of ERK1/2 on carbachol-induced axonal growth in hippocampal neurons. Hippocampal neurons plated on coverslips were treated with the ERK1/2 signaling pathway inhibitors U0126 or PD98059 (A) for 24 h. Cells were then fixed and stained with a β -tubulin antibody and a fluorescent secondary as described under *Materials and Methods*. The length of the axons was quantified using MetaMorph. The results derive from the measurements of 60 cells per treatment and are expressed as mean \pm S.E.M. (*, $p < 0.05$ versus control; #, $p < 0.05$ versus carbachol alone.) Hippocampal neurons electroporated in the absence of RNA, in the presence of nontarget siRNA, or in the presence of ERK1/2 siRNA were plated in 35-mm dishes for Western blot analysis of ERK1/2 levels (B and C) or on coverslips for morphological analysis (D). B, densitometric analysis of ERK1/2 levels normalized to control; the results shown are the average of three independent experiments (#, $p < 0.05$ compared with control). C, representative immunoblots of ERK1/2 levels in electroporated neurons. D, morphometric analysis of the effect of ERK1/2 siRNA on carbachol-stimulated axonal growth. The results derive from the measurements of 60 cells per treatment and are expressed as mean \pm S.E.M. (*, $p < 0.05$ compared with control. #, $p < 0.05$ compared with carbachol).

release of Ca^{2+} from intracellular stores and the activation of PKC and ERK1/2 play a primary role in the neuritogenic effect of carbachol in hippocampal neurons.

Carbachol Induces Ca^{2+} Mobilization and Activation of PKC and ERK1/2 in Hippocampal Pyramidal Neurons. We also tested the ability of carbachol to induce Ca^{2+} release and to activate PKC and ERK1/2 in cultures of hippocampal pyramidal neurons. To measure calcium mobilization, neurons were preincubated with the intracellular calcium indicator Fluo-3/AM. Images of the cells were captured every 10 s by an inverted fluorescent microscope attached to a digital camera. Carbachol (100 μM) was added to the cultures after 100 s of recording, and image capture continued for an additional 200 s; the Ca^{2+} -bound fluorescent Fluo-3/AM was subsequently quantified in at least 50 cells/experiment. Seventy percent of the cells (± 8.84) responded to carbachol with a rapid increase in intracellular Ca^{2+} that returned to control levels within 200 s. Figure 7A shows the average normalized fluorescence intensity before

and after carbachol treatment. EGTA (1 mM) did not inhibit carbachol-induced increase in intracellular Ca^{2+} , thereby confirming that this effect was because of the release of Ca^{2+} from intracellular stores (data not shown).

To measure PKC activation, a nonradioactive kit that quantifies the ability of PKC to phosphorylate a fluorescent substrate was used. Carbachol (100 μM) caused a significant increase in PKC activity after 15- and 30-min treatments (Fig. 7B). Morphometric experiments carried out in the presence of semiselective PKC inhibitors had suggested that the Ca^{2+} -dependent and/or -independent PKCs may be involved in the effect of carbachol on axonal growth (Fig. 5B). To test whether intracellular Ca^{2+} was involved in carbachol-induced PKC activation, we measured PKC activity in the presence of BAPTA-AM. We found that BAPTA-AM did not inhibit PKC activation by carbachol (Fig. 7C), whereas partially inhibiting PKC activation induced by phorbol 12-myristate 13-acetate, a potent activator of Ca^{2+} -dependent and Ca^{2+} -independent PKCs (Supplemental Fig. 2). The broad-

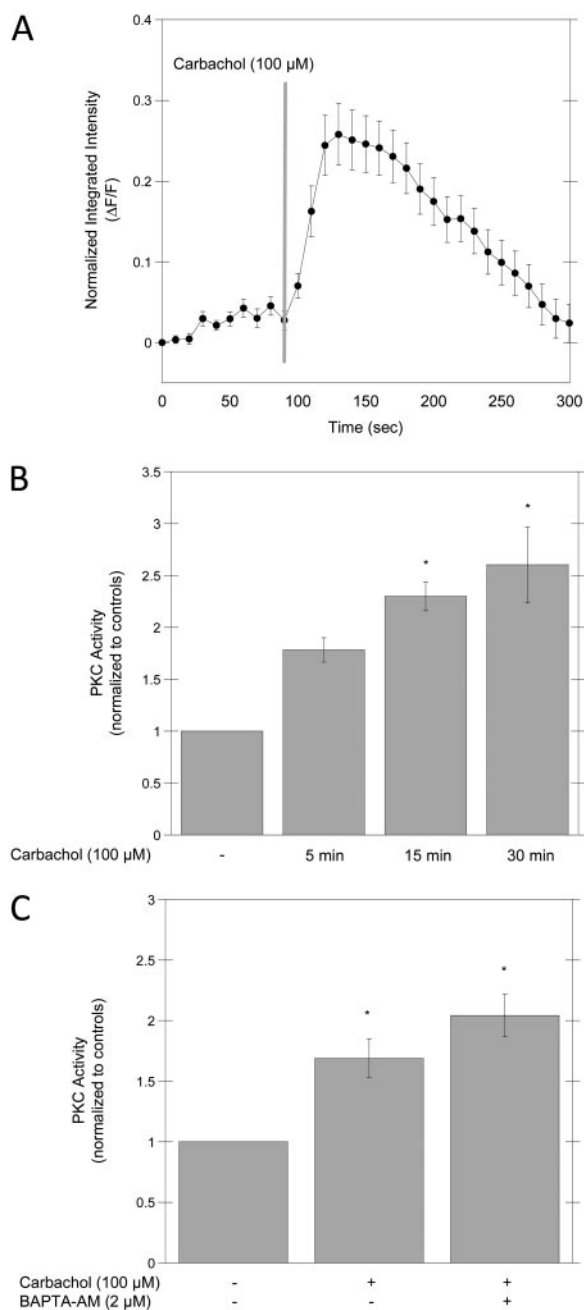


Fig. 7. Effect of carbachol on intracellular calcium mobilization and PKC activation. **A**, hippocampal neurons plated in 35-mm glass-bottomed dishes were loaded with the Ca^{2+} -sensitive fluorescent dye Fluo-3/AM and placed on the stage of an inverted fluorescence microscope. Images were captured at 10-s intervals, and carbachol (100 μM) was added after 100 s. Images were analyzed using MetaMorph. Fifty cells were analyzed, and fluorescence measurements were normalized as $\Delta F/F$. Similar results were obtained in three independent experiments. Hippocampal neurons were treated with carbachol (100 μM) for 5, 15, or 30 min (**B**) or for 15 min with carbachol in the presence of BAPTA-AM (2 μM) (**C**), and cell lysates were collected and equal amounts of proteins were incubated with a fluorescent PKC substrate as described under *Materials and Methods*. At the end of the reaction, the mixture was separated on an agarose gel, and the bands corresponding to the phosphorylated peptide were quantified and normalized to controls. The results shown are the average of three independent experiments (*, $p < 0.05$ compared with control).

spectrum PKC inhibitor GF109203X and the semiselective inhibitor Ro-32-0432 (which inhibits all the Ca^{2+} -dependent PKC plus PKC ϵ) completely inhibited PKC activation (Sup-

plemental Fig. 3), suggesting that PKC ϵ may be activated by carbachol in pyramidal hippocampal neurons.

Finally, we investigated the effect of carbachol on ERK1/2 phosphorylation in hippocampal pyramidal neurons by Western blot, using ERK1/2 phospho-specific antibodies. Densitometric analysis revealed that carbachol (100 μM) caused a 2-fold increase in the levels of phosphorylated (active) ERK1/2 in hippocampal neurons after 30-min incubation (Fig. 8A). Figure 8B shows representative immunoblots of phospho-ERK1/2, total ERK1/2, and β -actin in control and carbachol-stimulated neurons.

To understand whether intracellular calcium mobilization and PKC activation are involved in carbachol-stimulated ERK1/2 phosphorylation, hippocampal neurons were pretreated with BAPTA-AM or the pan-PKC inhibitor GF109203X before the addition of 100 μM carbachol for 30 min. GF109203X, but not BAPTA-AM, abolished the phosphorylation of ERK1/2 induced by carbachol (Fig. 8C), suggesting that the activation of a Ca^{2+} -independent PKC is required for carbachol-stimulated ERK1/2 phosphorylation.

Discussion

Previous studies reported that the activation of muscarinic receptors induces neuritogenesis in neuronal cell lines (Pinkas-Kramarski et al., 1992; De Jaco et al., 2002) and peripheral neurons (Tata et al., 2003). In this study, we described for the first time that carbachol stimulates axonal growth in CNS neurons through the activation of M_1 muscarinic receptors (Figs. 1–3), and we validated the evidence that acetylcholine may play a role in shaping the developing brain (Lauder and Schambra, 1999; Hohmann, 2003). In particular, we have shown that carbachol accelerated the elongation of the axon in pyramidal hippocampal and neocortical neurons, whereas it did not affect the length of neurites in CGCs (Figs. 2 and 4).

To better characterize the effect of carbachol on hippocampal neurons, we investigated the signal transduction pathways involved in this effect, and we identified the release of Ca^{2+} from intracellular stores and the activation of PKC and ERK1/2 as key events in carbachol-induced axonal growth. These results are in agreement with the notion that G_q -coupled receptors, such as M_1 muscarinic receptors, stimulate the activation of phospholipase C leading to the hydrolysis of phosphatidylinositides to IP_3 and DAG. IP_3 , through the interaction with specific receptors on the membrane of the endoplasmic reticulum, induces the release of Ca^{2+} , which is involved in the activation and regulation of numerous proteins, including Ca^{2+} -dependent PKCs. DAG is also an activator of PKCs (Sternweis and Smrcka, 1993), which, in turn, have been shown to activate ERK1/2 (Naor et al., 2000).

Our laboratory has reported previously that in astrocytes, which do not express M_1 muscarinic receptors, stimulation of M_3 receptors (also coupled to G_q proteins) induces the activation of additional pathways involving PLD, PI3K, the atypical PKC ζ , p70S6K, and NF- κB (Costa et al., 2001, 2004). Our results, however, suggest that these pathways are not relevant for the neuritogenic effect of M_1 muscarinic receptors in pyramidal hippocampal neurons.

We also verified that carbachol induced the release of Ca^{2+} from intracellular stores and activated PKC and ERK1/2 in hippocampal neurons (Figs. 6 and 7). However, the intracel-

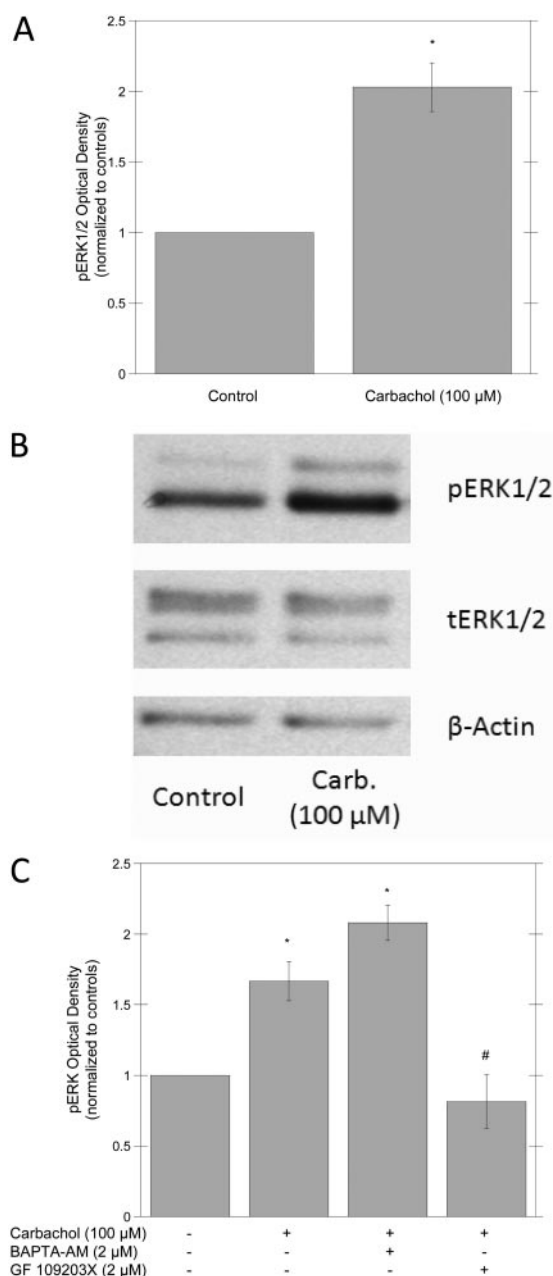


Fig. 8. Effect of carbachol on ERK1/2 activation. Hippocampal neurons were treated for 30 min in the presence of carbachol (100 μM); proteins were then extracted and analyzed by Western blot as described under *Materials and Methods*. **A**, optical densities of phosphorylated ERK1/2 normalized to controls; the results shown represent the average of three independent experiments (*, $p < 0.05$ compared with control). **B**, representative immunoblots of the effect of carbachol on ERK1/2 phosphorylation. **C**, hippocampal neurons were pretreated for 30 min with or without the intracellular calcium chelator BAPTA-AM (2 μM) or GF109203X (2 μM) followed by the addition of carbachol (100 μM) for an additional 30 min. Proteins were extracted and analyzed by Western blot as described under *Materials and Methods*. Graphs represent the average of three independent experiments (*, $p < 0.05$ compared with control; #, $p < 0.05$ compared with carbachol).

lular Ca²⁺ chelator BAPTA-AM, although inhibiting neurite outgrowth, did not inhibit PKC or ERK1/2 activation (Figs. 7C and 8C). Ca²⁺ has been implicated in axonal growth through mechanisms independent from PKC activation that involve its interactions with cell adhesion molecules and Ca²⁺/calmodulin-dependent kinases (Doherty et al., 2000;

Wayman et al., 2008). Thus, the lack of an effect of Ca²⁺ chelation on the activation of PKC and its downstream target ERK1/2 does not preclude its involvement on other aspects of axonal growth.

Data obtained using PKC inhibitors suggested that Ca²⁺-dependent PKC βII and γ and/or Ca²⁺-independent PKC ε may be involved in the neuritogenic effect of carbachol on hippocampal neurons (Fig. 5B). In contrast, PKC and ERK1/2 activation by carbachol was not affected by the chelation of intracellular Ca²⁺ (Figs. 7C and 8C), suggesting that PKC ε is the isoform involved in the effect of carbachol on ERK1/2 activation and axonal growth. These results are in agreement with previous studies reporting on the involvement of PKC ε in neurite outgrowth (Larsson, 2006).

Finally, our data strongly support the involvement of mitogen-activated protein kinase in carbachol-induced neurite outgrowth. Indeed, in addition to the data obtained with pharmacological inhibitors, we also found that the down-regulation of ERK1/2 by siRNA blocked the effect of carbachol (Fig. 6), in agreement with previous reports showing mitogen-activated protein kinase involvement in neurite outgrowth induced by nerve growth factor (Goold and Gordon-Weeks, 2005) and by the neural cell adhesion molecule L1 (Schmid et al., 2000).

In conclusion, we have shown that carbachol induces axonal growth in primary cultures of pyramidal neurons. This effect is mediated by the activation of M₁ muscarinic receptors that leads to the release of Ca²⁺ from intracellular stores and activation of PKC and ERK1/2.

Neuritogenesis involves the interplay of several factors, including extracellular matrix proteins (many of which are secreted by glial cells), cell adhesion molecules (which are expressed on the membranes of growing neurites and of “guiding” glial cells), and neurotrophic factors (soluble neuropeptides that interact with specific receptors on neurons and trigger the activation of intracellular signaling pathways leading to cytoskeleton protein rearrangement) (Kiryushko et al., 2004). We recently reported that the stimulation of M₃ muscarinic receptors in astrocytes induces minor neurite and axonal growth in hippocampal neurons coincubated with astrocytes after carbachol removal, by affecting the release of extracellular matrix proteins by astrocytes (Guizzetti et al., 2008). The present study showed that carbachol stimulates axonal growth when incubated directly with pyramidal neurons. Whether such an effect is mediated by increased transcription and/or release of the neuritogenic molecules described above, which can act in an autocrine manner on neurons, remains to be determined. Nevertheless, together this evidence suggests that muscarinic stimulation is a potent and complete inducer of neuritogenesis acting on both ends, directly on neurons by stimulating an intracellular signaling pathway and on astrocytes by affecting the secretion of guiding factors.

Because in our cell culture system hippocampal neurons, maintained for 24 h in vitro, have not developed synapses yet (Dotti et al., 1988), the reported effect of carbachol is extrasynaptic and is likely localized at the level of the growing axon. The concentrations of carbachol that induce neurite outgrowth are lower than the concentrations of acetylcholine found in synaptic vesicles (which are in the millimolar range) (Dunant and Israël, 2000). These lower concentrations are in agreement with our hypothesis that acetylcholine released by

growing axons before synaptogenesis occurs (Yao et al., 2000) may be responsible for neurogenesis of neighboring neurons in the developing brain.

These findings may be important for the understanding of the mechanisms behind the beneficial effects of perinatal choline supplementation observed in rodent models of fetal alcohol syndrome (Ryan et al., 2008) and Rett syndrome (Ward et al., 2008), because in both these conditions alterations in the cholinergic system have been proposed (Costa et al., 2001; Ward et al., 2008). In addition, neurite regeneration and repair after neuronal damage may be compromised in certain pathological conditions that cause loss of cholinergic neurons, such as Alzheimer's disease (Bartus et al., 1982).

Acknowledgments

We thank Khoi Dao and Daniella Pizzurro for assistance with some of the experiments.

References

- Barbin G, Pollard H, Gaiarsa JL, and Ben-Ari Y (1993) Involvement of GABAA receptors in the outgrowth of cultured hippocampal neurons. *Neurosci Lett* **152**:150–154.
- Bartus RT, Dean RL 3rd, Beer B, and Lippa AS (1982) The cholinergic hypothesis of geriatric memory dysfunction. *Science* **217**:408–414.
- Bearer CF, Swick AR, O'Riordan MA, and Cheng G (1999) Ethanol inhibits L1-mediated neurite outgrowth in postnatal rat cerebellar granule cells. *J Biol Chem* **274**:13264–13270.
- Berger-Sweeney J (2003) The cholinergic basal forebrain system during development and its influence on cognitive processes: important questions and potential answers. *Neurosci Biobehav Rev* **27**:401–411.
- Bradford MM (1976) A rapid and sensitive method for the quantitation of microgram quantities of protein utilizing the principle of protein-dye binding. *Anal Biochem* **72**:248–254.
- Brewer GJ, Torricelli JR, Evege EK, and Price PJ (1993) Optimized survival of hippocampal neurons in B27-supplemented Neurobasal, a new serum-free medium combination. *J Neurosci Res* **35**:567–576.
- Costa LG, Guizzetti M, Oberdoerster J, Yagle K, Costa-Mallen P, Tita B, Bordi F, Vitalone A, Palmery M, and Valeri P (2001) Modulation of DNA synthesis by muscarinic cholinergic receptors. *Growth Factors* **18**:227–236.
- Costa LG, Vitalone A, and Guizzetti M (2004) Signal transduction mechanisms involved in the antiproliferative effects of ethanol in glial cells. *Toxicol Lett* **149**:67–73.
- De Jaco A, Augusti-Tocco G, and Biagioni S (2002) Muscarinic acetylcholine receptors induce neurite outgrowth and activate the synapsin I gene promoter in neuroblastoma clones. *Neuroscience* **113**:331–338.
- DeFelipe J and Fariñas I (1992) The pyramidal neuron of the cerebral cortex: morphological and chemical characteristics of the synaptic inputs. *Prog Neurobiol* **39**:563–607.
- Doherty P, Williams G, and Williams EJ (2000) CAMs and axonal growth: a critical evaluation of the role of calcium and the MAPK cascade. *Mol Cell Neurosci* **16**:283–295.
- Dotti CG, Sullivan CA, and Banker GA (1988) The establishment of polarity by hippocampal neurons in culture. *J Neurosci* **8**:1454–1468.
- Dunant Y and Israël M (2000) Neurotransmitter release at rapid synapses. *Biochimie* **82**:289–302.
- Giordano G, White CC, McConnachie LA, Fernandez C, Kavanagh TJ, and Costa LG (2006) Neurotoxicity of domoic acid in cerebellar granule neurons in a genetic model of glutathione deficiency. *Mol Pharmacol* **70**:2116–2126.
- Goold RG and Gordon-Weeks PR (2005) The MAP kinase pathway is upstream of the activation of GSK3beta that enables it to phosphorylate MAP1B and contributes to the stimulation of axon growth. *Mol Cell Neurosci* **28**:524–534.
- Guizzetti M, Costa P, Peters J, and Costa LG (1996) Acetylcholine as a mitogen: muscarinic receptor-mediated proliferation of rat astrocytes and human astrocytoma cells. *Eur J Pharmacol* **297**:265–273.
- Guizzetti M, Moore NH, Giordano G, and Costa LG (2008) Modulation of neurogenesis by astrocyte muscarinic receptors. *J Biol Chem* **283**:31884–31897.
- Hohmann CF (2003) A morphogenetic role for acetylcholine in mouse cerebral neocortex. *Neurosci Biobehav Rev* **27**:351–363.
- Karczmar AG (2007) *Exploring the Vertebrate Central Cholinergic Nervous System*, Springer, New York.
- Kiryushko D, Berezin V, and Bock E (2004) Regulators of neurite outgrowth: role of cell adhesion molecules. *Ann NY Acad Sci* **1014**:140–154.
- Larsson C (2006) Protein kinase C and the regulation of the actin cytoskeleton. *Cell Signal* **18**:276–284.
- Lauder JM and Schambra UB (1999) Morphogenetic roles of acetylcholine. *Environ Health Perspect* **107** (Suppl 1):65–69.
- Lohmann C, Myhr KL, and Wong RO (2002) Transmitter-evoked local calcium release stabilizes developing dendrites. *Nature* **418**:177–181.
- Matsutani S and Yamamoto N (1998) GABAergic neuron-to-astrocyte signaling regulates dendritic branching in coculture. *J Neurobiol* **37**:251–264.
- Mattson MP, Dou P, and Kater SB (1988) Outgrowth-regulating actions of glutamate in isolated hippocampal pyramidal neurons. *J Neurosci* **8**:2087–2100.
- Michler A (1990) Involvement of GABA receptors in the regulation of neurite growth in cultured embryonic chick tectum. *Int J Dev Neurosci* **8**:463–472.
- Naor Z, Benard O, and Seger R (2000) Activation of MAPK cascades by G-protein-coupled receptors: the case of gonadotropin-releasing hormone receptor. *Trends Endocrinol Metab* **11**:91–99.
- Pearce IA, Cambray-Deakin MA, and Burgoyne RD (1987) Glutamate acting on NMDA receptors stimulates neurite outgrowth from cerebellar granule cells. *FEBS Lett* **223**:143–147.
- Pinkas-Kramarski R, Stein R, Lindenboim L, and Sokolovsky M (1992) Growth factor-like effects mediated by muscarinic receptors in PC12M1 cells. *J Neurochem* **59**:2158–2166.
- Priest CA and Puche AC (2004) GABAB receptor expression and function in olfactory receptor neuron axon growth. *J Neurobiol* **60**:154–165.
- Ryan SH, Williams JK, and Thomas JD (2008) Choline supplementation attenuates learning deficits associated with neonatal alcohol exposure in the rat: effects of varying the timing of choline administration. *Brain Res* **1237**:91–100.
- Schmid RS, Pruitt WM, and Maness PF (2000) A MAP kinase-signaling pathway mediates neurite outgrowth on L1 and requires Src-dependent endocytosis. *J Neurosci* **20**:4177–4188.
- Schwamborn JC, Li Y, and Püschel AW (2006) GTPases and the control of neuronal polarity. *Methods Enzymol* **406**:715–727.
- Smit M, Leng J, and Klemke RL (2003) Assay for neurite outgrowth quantification. *Biotechniques* **35**:254–256.
- Song JH, Wang CX, Song DK, Wang P, Shuaib A, and Hao C (2005) Interferon gamma induces neurite outgrowth by up-regulation of p35 neuron-specific cyclin-dependent kinase 5 activator via activation of ERK1/2 pathway. *J Biol Chem* **280**:12896–12901.
- Sternweis PC and Smreka AV (1993) G proteins in signal transduction: the regulation of phospholipase C. *Ciba Found Symp* **176**:96–106; discussion 106–111.
- Tata AM, Cursi S, Biagioni S, and Augusti-Tocco G (2003) Cholinergic modulation of neurofilament expression and neurite outgrowth in chick sensory neurons. *J Neurosci Res* **73**:227–234.
- Tessier-Lavigne M and Goodman CS (1996) The molecular biology of axon guidance. *Science* **274**:1123–1133.
- Ward BC, Agarwal S, Wang K, Berger-Sweeney J, and Kolodny NH (2008) Longitudinal brain MRI study in a mouse model of Rett Syndrome and the effects of choline. *Neurobiol Dis* **31**:110–119.
- Wayman GA, Lee YS, Tokumitsu H, Silva A, and Soderling TR (2008) Calmodulin-kinases: modulators of neuronal development and plasticity. *Neuron* **59**:914–931.
- Whitworth TL, Herndon LC, and Quick MW (2002) Psychostimulants differentially regulate serotonin transporter expression in thalamocortical neurons. *J Neurosci* **22**:RC192.
- Yao WD, Rusch J, Poo M, and Wu CF (2000) Spontaneous acetylcholine secretion from developing growth cones of *Drosophila* central neurons in culture: effects of cAMP-pathway mutations. *J Neurosci* **20**:2626–2637.

Address correspondence to: Dr. Marina Guizzetti; Department of Environmental and Occupational Health Sciences, University of Washington, 4225 Roosevelt Way NE Suite 100, Seattle, WA 98105. E-mail: marinag@u.washington.edu